JOURNAL OF PROPULSION AND POWER
Vol. 14, No. 4, July–August 1998

Measurement System for Determining Solid Propellant Burning Rate Using Transmission Microwave Interferometry

Vladica S. Bozic,* Djordje D. Blagojevic,† and Bozidar A. Anicin‡
Belgrade University, Belgrade 11000, Yugoslavia

A new and unique measurement system is presented, based on microwave transmission interferometry. The system has been developed after successful experiments with reflection microwave interferometry and operates in the K_a-band (35 GHz). It is used for the direct and continuous measurement of the instantaneous burning rate of solid rocket propellants at different pressures and different gas flows over the burning surface in a solid rocket motor. The system consists of an experimental motor, microwave installation, hardware, and special software for data reduction. The software yields burning-rate data immediately after test runs. The principle of the measurement method and data reduction is given in this paper, together with a description of the test motor and microwave installation. Base and erosive burning rates are given for three types of ammonium perchlorate–polyvinyl chloride-based composite rocket propellant formulations. The results demonstrate that the transmission microwave interferometry system is a reliable tool for nonintrusive determination of instantaneous burning surface location of a center-perforated cylindrical propellant grain.

Nomenclature

A_e = throat cross-sectional area for erosive nozzle
A_{kr} = throat cross-sectional area of all nozzles
A_p = flow area, cross-sectional area inside the internal perforation of a measuring pill where instantaneous mass flow is determined
b = coefficient of pressure in the Saint–Robert's law of burning rate
C^* = characteristic velocity
d_p = diameter of the internal perforation of a measuring pill
G = mass flux
I_p = total pressure impulse
m = mass flow through all nozzles
m_p = instantaneous mass flow through the measuring pill
n = pressure exponent of burning rate in the Saint–Robert's law
n_r = index of refraction of propellant at the operating wavelength
P_c = combustion pressure
r = $r_e + r_0$, burning rate of propellant under given conditions of pressure, propellant temperature, and gas flow
r_e = erosive propellant burning rate
r_0 = base burning rate, burning rate of propellant under same conditions of pressure and propellant temperature, but with no gas flow
t = time
ΔD = change of measuring pill diameter
ΔM = mass exhausted through all nozzles
ΔQ = standard deviation of the burning rate in comparison with Saint–Robert's law
$\Delta\phi$ = change of phase of the microwave signal
ε = erosion ratio, r/r_0
λ_0 = free-space wavelength

Subscript
(t) = instantaneous value

Introduction

ACCURATE knowledge of the burning rate of a solid propellant is a prerequisite in the design of new solid propellant rocket motors. The burning mechanism is very complex and involves a large number of chemical and physical processes. The burning rate of solid propellants depends on a number of parameters: the pressure and the initial propellant temperature, crossflow velocity, propellant type, fuel-to-oxidizer ratio, and oxidizer particle size in the case of composite propellants. Generally, the burning rates of solid propellants may be described by the empirical equation (Saint–Robert's law):

$$r = bP_c^n \tag{1}$$

It was established in the early days of solid rocket motor development that grains with an interior channel yield higher burning rates than flat grains. This phenomenon was attributed to the flow of combustion products over the burning surface. In the literature the effect of modification of burning rates by the flow is called erosive burning. The erosive burning of solid propellants results from increased transfer of heat toward the burning zone because of flow. It depends on the interaction between the propellant burning characteristics and the details of the flow (mass flow rate, velocity gradient near the surface, and geometric configuration). The burning rate usually increases with an increase in gas velocity. The erosive component of burning rate is the difference between the burning rate in the presence of flow and the base burning rate at the same burning pressure and initial temperature of propellant.

From the moment this phenomenon was established, numerous successful methods have been developed for erosive burning-rate measurements of solid rocket propellants. All of these methods can generally be divided into two main groups: 1) laboratory sample methods and 2) direct motor firing methods. Laboratory sample methods can be used only on labora-

Received May 2, 1997; presented as Paper 97-2842 at the AIAA/ASME/SAE/ASEE 33rd Joint Propulsion Conference, Seattle, WA, July 6–9, 1997; revision received Nov. 17, 1997; accepted for publication Dec. 4, 1997.

*Research Assistant, Faculty of Mechanical Engineering; currently at Infinity, Djure Djakovica 8, Zemun, Serbia, Yugoslavia.
†Associate Professor, Faculty of Mechanical Engineering; currently at Infinity, Djure Djakovica 8, Zemun, Serbia, Yugoslavia.
‡Professor (Retired).

tory test motors and include x rays,[1,2] photographic,[3,4] laser photodiode servomechanisms,[5] and ultrasonic methods.[6] Direct motor firing methods can be used on real motors and also on test motors. This group involves methods of interrupted burning,[1,7] conductivity, ionization,[8] and thermocouple probes.

Previous Investigations

In the propellant industry microwave techniques have been used for a long time for burning-rate measurements in rocket motors. The first paper in which the use of microwaves was mentioned is the paper by Koch,[9] in which the use of microwaves to measure detonation velocities in explosives was described. The first paper on the microwave measurement of regression rates in solid propellants is by Johnson.[10] Further contributions to microwave burning-rate measurements are those by Dean and Green[11] and Wood et al.[12] Microwave techniques were widely used for measurement of solid propellant burning rates under steady and oscillatory conditions, as described in the papers by Gittins et al.,[13] Alkidas et al.,[14] and Strand et al.[15,16]

At the Jet Propulsion Laboratory of the Faculty of Mechanical Engineering in Belgrade, in a period of over 15 years, different microwave installations and different methods of data reduction have been used to determine burning rates of solid rocket propellants. Experimental investigations aimed to develop a method for determining solid rocket propellant burning rate along the internal perforation of a cylindrical propellant grain have been made possible after the successful development of a measurement system for determining solid propellant burning rate using reflection microwave interferometry[17] and transmission experiments.[18] The method is based on microwave transmission interferometry. It appears from the literature that this is the very first attempt of using transmission microwave interferometry for burning-rate measurement.

Transmission experiments have been performed to investigate possible effects of the transient flame zone ionization level on the burning rate determined by the microwave technique.[18] It was shown that the passage of microwaves through flames approximately 1 cm thick does not produce the slightest change in wave amplitude. The complete absence of any flame plasma effects in reflection experiments was also established. Although this is at variance with a very common point of view in the early history of the method, it agrees with the concepts that evolved in the mature phase of the method's development.[14] The reason for the virtual absence of flame plasma effects is the low electron density at the flame temperatures encountered in the propellants used in the experiments. The electron density is low when compared to the very high critical electron density corresponding to the microwave operating frequency (1.510^{13} electrons/cm^3).

These experiments show that the flame of the propellant does not reflect or absorb a large part of the microwave power, and that it has no significant effect in microwave measurements. The influence of the flame plasma is taken to be completely negligible. The reflection signal is actually formed from the propellant/gas phase interface.

Principle of Microwave Transmission Interferometry

The determination of burning rates by microwave transmission interferometry is based on the phenomenon of partial reflection and transmission of electromagnetic waves, incident at the interface between two different dielectric mediums (solid propellant and gases combustion products at burning surface in this case). When a microwave signal reaches the burning surface of propellant, reflected and transmitted waves are formed from an incident wave. As the burning surface moves during the combustion process, both waves exhibit continual changes in phase. These changes in phase can be used to determine the position of the burning surface and, therefore, burning rate. The method described in this paper uses the microwave signal transmitted through the contact surface of propellant and the gas products of combustion.

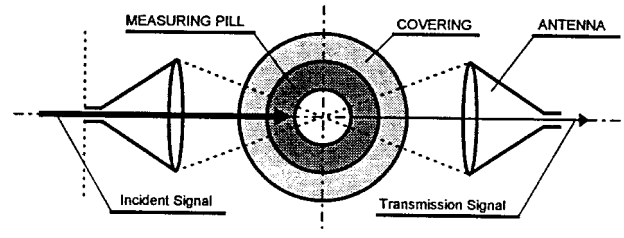

Fig. 1 Microwave burning-rate measurement technique.

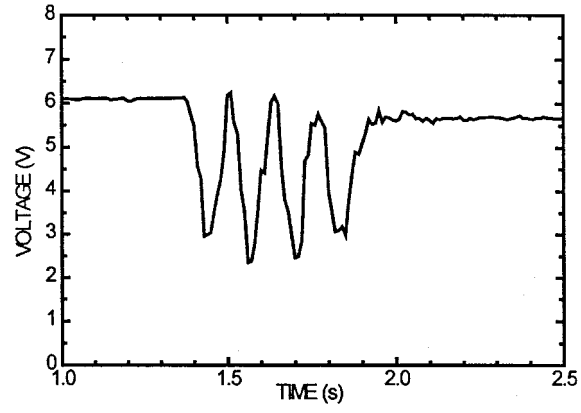

Fig. 2 Interference pattern from one erosive test with composite propellant *C*.

The principle of burning-rate measurement using microwave transmission interferometry is illustrated in Fig. 1. In many elements, it is similar to reflection microwave interferometry. Electromagnetic radiation from the generator is divided by a microwave installation into two parts. One part of the electromagnetic radiation is propagated through a lateral branch of the microwave installation to produce a signal of constant phase. This part of the radiation is called the reference signal and the respective part of the installation is called the reference branch. A second part of the electromagnetic radiation propagates through a cylindrical propellant sample (measuring pill), which is put in an appropriate covering and placed together with it in the combustion chamber. Electromagnetic radiation is both reflected and transmitted at each material interface. This part of the microwave installation is called the measurement branch. The signal of interest is the transmission signal that emerges from the opposite side of the measuring pill. This signal changes continuously in phase during the regression of the burning surface. The transmission signal is then merged with a reference signal to form a new wave. The transmission signal and the reference signal alternatively reinforce and destroy each other when they are superposed, and this process is generally termed interferometry. This new wave is received by a detector, which transforms microwave power into electric current and voltage. The detector signal is a sine wave, and the phase of this sine wave changes with reduction in thickness of the burning sample (Fig. 2). The voltage signal is steady in the absence of burning. The distance between two adjacent maxima or minima in this signal is proportional to the wavelength of the signal in the propellant. It defines the position of the burning surface in time, and combined with appropriate methods of data reduction makes possible the calculation of the value of the burning rate and mass flow.

Assuming that the application of ray optics to the system in Fig. 1 is justifiable, the $\Delta\phi$ is proportional to ΔD:

$$\Delta\phi = (2\pi/\lambda_0)\cdot(n_r - 1)\cdot\Delta D \qquad (2)$$

Now, in practice, the diameter of the propellant bore is several wavelengths. This opens the question of the applicability of ray optics. Furthermore, the lenses are not of infinite extent normal to the plane of the paper, but rotationally symmetric around the beam axis. All of this presents a formidable problem in full-wave electromagnetic theory. Fortunately, the problem was dealt with experimentally in microwave plasma diagnostics[19] in an experiment known as the inverted world experiment. In this experiment, which is similar to our experiment shown in Fig. 1, microwaves were passed through paraffin blocks with central bores of different diameters, and negligible departures from Eq. (2) were recorded, provided the bore diameter is at least three free-space wavelengths of the radiation.

The solid rocket propellant measuring pill does not have enough strength to endure difficult working conditions. To provide greater strength, a covering is placed around the measuring pill. This covering adds additional reflected and transmitted signals between the measuring pill and air at both sides of the microwave signal path. To keep this effect to a minimum we have selected a plastic covering with dielectric properties between those of propellant and air, with a thickness equal to an odd number of half wavelengths in the material.

Data Reduction Method

The existence of reflections makes the determination of regression rates more complicated and the resulting burning rate is less accurate. It is necessary to remove these additional reflections from the detector signal if we wish to obtain good results. Reflections can be eliminated in large part by filtering during data reduction. Filtering also decreases the noise level and the effects of instantaneous instability in the burning process. The interference signal is first observed in the time domain to determine the interval for filtering. Filtering is performed with a digital bandpass filter. To eliminate the influence of test motor ignition, the signal is analyzed only in an interval of stable motor operation. After filtering, the clean signal is obtained where the influence of reflections and other noise is reduced to a minimum. This signal is used for additional data reduction to obtain burning-rate data independent of pressure and mass flux.

The reduction of data was based on the fact that the interferogram proved symmetric within the half-period, so that both minima and maxima of the fringe pattern were used. The distance between two adjacent maxima or minima of this signal is proportional to the wavelength of the signal in the propellant. As the propellant thickness changes, the distance between maxima also changes. This distance, supplemented by the distances of five points between each two maxima and minima with a phase difference of 30 deg directly yields the position of the burning surface at a particular time in terms of the propellant wavelength, known from the propellant refractive index that was measured separately. In this way it is possible to obtain a large number of burning surface positions at different pressures and mass fluxes in a single test. To avoid the accumulation of error that would result if differences of the primary data were formed, a polynomial was fit through several adjacent points of the thickness–time data, and the burning rate was determined as the derivative of the polynomial using the Savitzky and Golay method.[20]

The experimental accuracy is difficult to assess. Formally, the error should be composed according to Eq. (2). It is very difficult to establish the uncertainty in phase change, which was greatly reduced by the process of signal filtering. The accuracy of the burning-rate measurements depends on the accurate knowledge of the microwave wavelength in the solid propellant. The frequency of the microwave radiation was measured with an accuracy of $\pm 0.25\%$, and the index of refraction of propellant was determined with an accuracy of $\pm 1\%$, and the total error is equal to the sum of these two errors. Regarding reflection microwave interferometry, the results are dependent on the following factors: roughness of burning surface, grain compressibility, and transient flame ionization level. A detailed analysis of the influence of these factors upon reflection microwave interferometry was performed in Ref. 17. The results showed that these factors do not have a significant effect on the measured signal, and in this way, on the burning-rate results. Because of the similarity between the reflection and transmission microwave interferometry methods, the same conclusion can be applied to a transmission microwave interferometry system. Waesche and O'Brien[21] studied the operation of nozzleless motors and also discussed the relative merits of microwave measurement.

In erosive burning-rate measurements, apart from the obvious combustion chamber pressure measurement, it is necessary to determine G. Mass flux is determined in the measuring pill, at the same place where the burning rate is measured. It is defined with the following equation:

$$G_{(t)} = m_{p_{(t)}}/A_{p_{(t)}} \tag{3}$$

The instantaneous flow through a cross section of the measuring pill is defined with the following equation:

$$m_{p_{(t)}} = (P_{c(t)} \cdot A_{e_{(t)}})/C^* \tag{4}$$

where the instantaneous pressure in a combustion chamber is measured during the test and is changeable with time. Throat cross-sectional area for erosive nozzle is constant if ablation or sedimentation do not exist at the nozzle throat.

The characteristic velocity is

$$C^* = (P_c \cdot A_{kr})/m \tag{5}$$

It is impossible to measure the characteristic velocity directly with solid propellant. In this case, the characteristic velocity is calculated after a test. As all parameters vary with time, Eq. (5) is integrated with time to obtain the following:

$$C^* = \frac{\int_{(t)} P_{c_{(t)}} \cdot A_{kr_{(t)}} \cdot \mathrm{d}t}{\int_{(t)} m_{(t)} \cdot \mathrm{d}t} = \frac{I_p \cdot A_{kr}}{\Delta M} \tag{6}$$

The integral of chamber pressure during the total burn time is the total pressure impulse obtained from the pressure–time curve measured during the test. The integral of mass flow through all nozzles is the total mass exhausted through all nozzles. Theoretically, it is the mass of flow from the propellant. Practically, it is the difference in mass of the experimental motor before and after the test.

The experimental motor was fitted with two nozzles: the gas-generator and erosive nozzle. The throat cross-sectional area of these nozzles is determined with direct measurements of throat diameter before and after the test. If these diameters are constant, this area is also constant during the whole of motor operation. If the throat diameter changes, as a result of ablation or sedimentation of exhaust particles, it is assumed that this change is linear during the test.

Having determined the characteristic velocity from Eq. (6), the instantaneous mass flow through a cross section in the middle of the measuring pill, where the burning rate is measured is calculated from Eq. (4). The instantaneous flow area is determined from the measured port diameter of the measuring pill. The instantaneous port diameter is equal to the sum of the initial port diameter and two times the burned propellant thickness. The knowledge of the instantaneous flow area and instantaneous mass flow through the measuring pill makes the computation of the mass flux from Eq. (3) possible. As the

mass flow rate through a measuring pill is almost constant because of the nearly constant burning area of the gas-generating charge, and the cross-sectional area increases during burning, the mass flux decreases during the test. The burning rate together with the mass flux is measured during the test at an almost constant pressure. The base burning rate can be measured in the same experimental motor using the same method, in conditions without mass flow through the measuring pill. These data are combined to determine the influence of mass flux on erosive burning rate of the solid propellant.

Experimental Test Apparatus

The microwave installation is shown in block diagram form in Fig. 3. A continuous microwave signal is generated from a Gunn microwave oscillator fed from a Gunn bias regulator. It produces approximately 100 mW of microwave power with a 10-V, 1.7-A dc input. The oscillator is set at 35 GHz (K_a-band). A ferrite isolator is placed immediately at the oscillator output flange. The ferrite allows signal propagation in the forward direction only, preventing unwanted reflections of microwave radiation from other parts of the installation to reach the generator. The direct reading frequency meter placed behind the isolator measures the frequency of the input signal before each test.

The signal then passes through a variable attenuator that allows control of microwave power by movement of a resistive vane. The signal with an adjusted level of radiation enters the H arm of a hybrid tee junction (magic tee). In the magic tee, it is divided into two equal signals with half the power and with the same phase, one in each arm. One signal is directed to the experimental motor by a waveguide section. It reaches the transmitting horn lens antenna, with lenses made from poly(methyl methacrylate). This element focuses the radiation that passes radially through the covering and measuring pill and arrives at the receiving horn lens antenna. During the burning of the measuring pill the phase and intensity of the signal change. This signal, which carries the relevant information about the burning rate, is led by a rectangular waveguide to another magic tee. This is the measurement branch.

The other signal in the second arm of the magic tee, the reference signal, arrives there via a precision level-set attenuator and variable phase shifter. A precision level-set attenuator, placed behind the magic tee, allows control of the microwave power level of the signal that leaves this part of the installation. The variable phase shifter serves to set the phase of the signal precisely. This branch is known as the reference branch, because the signal is not changed in phase and amplitude. The phase regulator and precision attenuator are set before each test. This setting brings both waves (in the measurement and reference branch) to constructive interference, which makes the microwave interference signal start from a maximum. In this way we are certain that all subsequent points will stay within the data-acquisition range. This simplifies the measurements and helps subsequent data reduction. The magic tee is used again to couple and superpose the measurement and reference signals from both arms. The superposition of these two signals exits from the E arm of the magic tee and passes through an isolator (which serves to prevent possible unwanted reflections), to the tunable broadband detector with a silicon whisker contact diode. It converts microwave power into electric current and voltage that exhibits minimum sensitivities of up to 1500 mV/mW across the full waveguide bandwidth. All of these elements of the microwave installation are connected with a standard copper rectangular K_a-band waveguide. Terminations are placed at the free arms of both magic tees to absorb microwave radiation formed by reflection in various parts of the installation and prevent these reflections from reaching the detector.

The detector voltage is amplified 100 times and digitized by a computer, where it is recorded and stored on the computer's disk together with pressure-time data. In this way all of the data are in digital form convenient for recording, analysis, transfer, and storage. Also, microwave signal (burning rate) vs time data are coordinated with pressure vs time data.

The personal-computer-based data acquisition system used in the experiments consists of pressure transducers, charge amplifiers, microwave signal amplifier, elements for transfer of signals, A/D converter, personal computer (IBM PC or close compatible), control section, and pyrotechnic device controller. The test control, monitoring, data acquisition and reduction are performed on the personal computer. Programs for test control and data acquisition are specially developed for these types of tests. These programs store all data on disk for off-line data analysis.

The program for test data reduction and analysis reads all of the data (microwave signal and pressure) stored on disk, recalculates them from bytes to physical units using transducer data, and reads data analysis requirements (from a descriptor file or interactively). All of the data are smoothed by the modified Savitzky and Golay third-order N-point smooth and number reduction method and/or filter (Nth-order variable frequency Butterworth filter).[20] The smoothed microwave signal is spectrally analyzed using the fast Fourier transform (FFT) and filtered by a bandpass filter. Filtered data are transformed from the frequency domain to the time domain by the inverse FFT. At the end of this process an interferogram is obtained

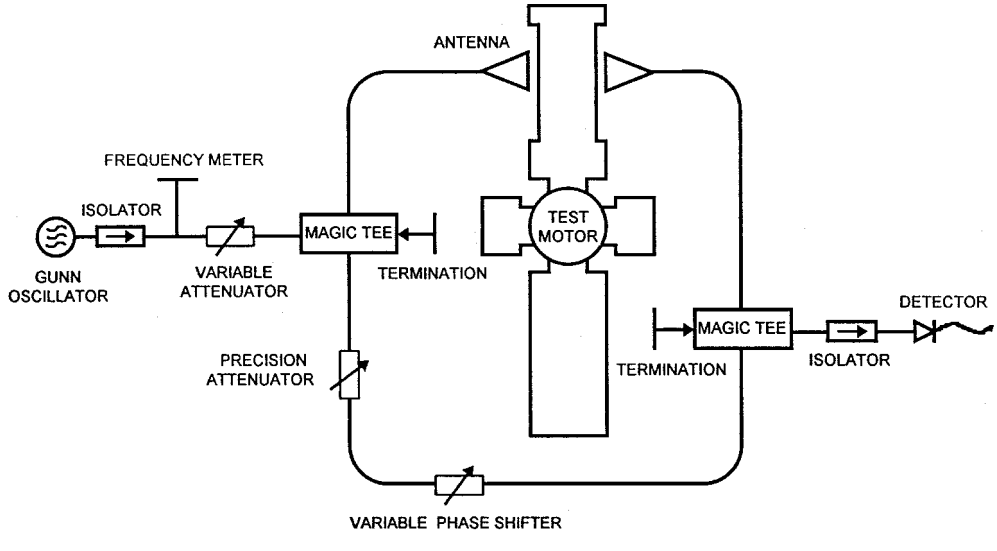

Fig. 3 Block diagram of the microwave measurement system.

in which unwanted multiorder reflections are removed leaving only the signal of the main transmission from burning surface/gas-phase interface. The position of the burning surface is calculated from the interferogram using the fact that the distance between two maxima or two minima corresponds to the half wavelength of the electromagnetic wave propagating in the propellant. The position of all extremes in the time domain is determined by calculation. The same calculation determines five points between two adjacent extremes with a phase difference of 30 deg. The change of position of the burning surface in time is obtained in this way. The burning rate of the examined propellant in a time domain is obtained by differentiating these data using the Savitzky and Golay third-order, seven-point differentiation. These burning-rate values in the time domain are transferred to the pressure domain to obtain the burning-rate law (dependence of burning rate on pressure). It is possible to calculate the specific mass flow rate in the time domain in a way described in the Data Reduction Method section of this paper.

The test motor is designed to yield combustion product gas temperature, pressure, and freestream velocity typical of solid propellant motors with internal burning cylinder grain. All basic elements are made of steel, capable of sustaining a number of tests. A schematic diagram of the test motor is presented in Fig. 4. The test motor consists of a central section and four additional sections: gas-generating section, nozzle, measuring, and membrane section. A special gas-generating charge burning in the gas-generating section forms a high-pressure hot-combustion gas flow needed to provide working pressure, temperature, and mass flow in the measuring section. This hot combustion gas simulates actual rocket conditions. Depending on the type of measurement performed, two different gas-generating chambers and propellant grains are used. When only the influence of pressure on burning rate is measured, the cylindrical propellant grain is inhibited at both ends and the outer lateral surface, producing a progressive burning surface. This makes burning-rate measurements possible over a range of pressures in a single test. The pressure range is up to 1:3. When the erosive burning rate is measured, the gas-generating chamber is three times longer. The cylindrical propellant grain is inhibited only at both ends producing a neutral burning surface development. This produces an almost constant pressure and a large and constant mass flow. The flame temperature and characteristic velocity of the measuring pill can be the same as that of the propellant grain when both are made from the same propellant composition.

The measuring section is placed opposite to the gas-generating section, between two horn-lens antennas. It consists of a case containing the measuring pill with a covering and the erosive nozzle with its support. Two ports on the body of the case serve to transmit microwave radiation from one antenna through the covering and measuring pill to the other antenna. The covering, in the shape of a hollow cylinder, is placed around the measuring pill. It allows easy transmission of microwave radiation from the transmitting to the receiving antenna through the measuring pill, and also provides greater strength of the whole motor construction. The measuring pill is a short laterally inhibited cylindrical grain, inhibited also from one head; its o.d. is 50 mm; its web is equal to or larger than the gas-generating charge web; and it is made from the same type of propellant whose burning rate is measured. During testing, the surface of the internal perforation is burning and decreases the web. This changes the phase and intensity of the microwave signal passing through the pill. The erosive nozzle is placed immediately behind the measuring pill in an appropriate support. It is made from molybdenum, whereas the support is made from copper. Various nozzles, with throat diameters from 5 to 16 mm, are used. A rubber cork is placed into the nozzle throat. When this nozzle is closed, no mass flow exits through the measuring pill. The burning rate is then measured only as a function of pressure. When the nozzle is opened, depending on the throat diameter, the mass flow of gas products passes through the measuring pill and produces erosive burning.

Convergent interchangeable exit nozzles that are mounted in the nozzle section were designed to provide the desired combustion pressure in the test chamber. As for the erosive nozzle and its support, the nozzle bodies are made of copper because of its good thermal capacity. To completely eliminate the possibility of ablation of the throat, a nozzle insert made of mo-

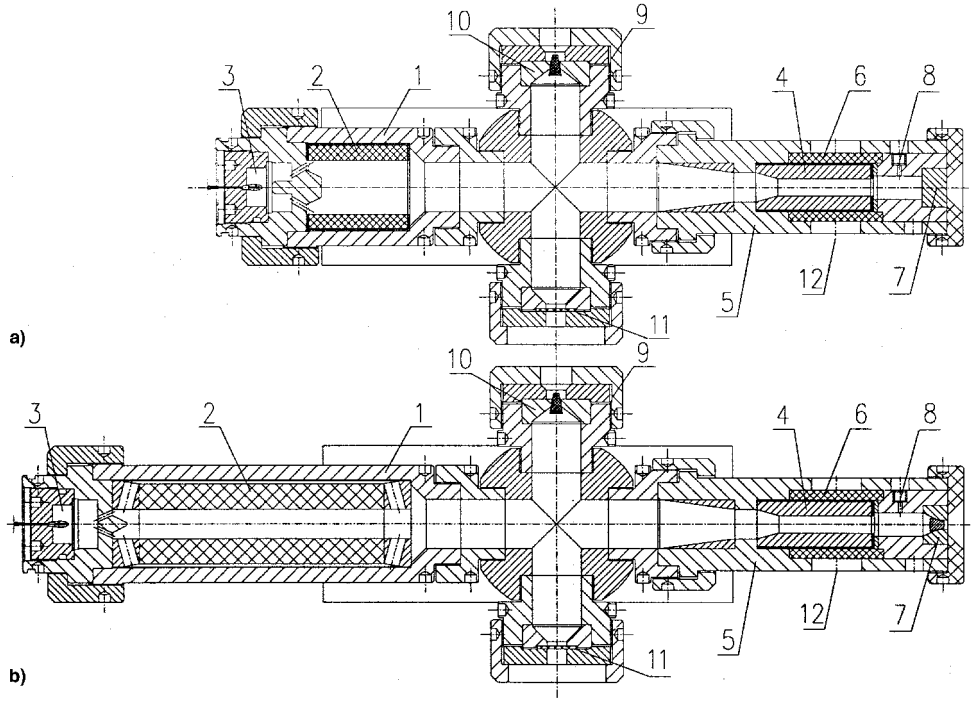

Fig. 4 Test motor assembly. Configurations for a) base and b) erosive burning measurements. 1, chamber of the gas-generating section; 2, gas-generating charge; 3, igniter; 4, measuring pill; 5, chamber of the measuring section; 6, covering; 7, erosive nozzle; 8, pressure transducer port; 9, nozzle section; 10, exit nozzle; 11, membrane section; and 12, microwave viewing port.

lybdenum is placed into it. The use of molybdenum ensures a fixed throat area during all burning processes. Various nozzles, with throat diameters from 5 to 16 mm, were used. A combination of different throat diameters in erosive and exit nozzles before the test secures desired values of combustion pressure and mass flow in the measuring pill.

To facilitate the ignition process in the combustion chamber, a rubber cork is placed into both nozzle throats. This cork serves as a membrane and facilitates the buildup of working pressure in the combustion chamber. The dimensions of the cork correspond to the diameter of the nozzle throat. The cork is pushed out of the nozzle at some definite high pressure, and from that moment the motor operates normally.

A safety valve of the membrane type is placed in the membrane section opposite to the nozzle section, to prevent destruction of the entire motor in case of high pressure during testing. If the pressure in the combustion chamber exceeds 20 MPa, the membrane is destroyed. In this manner the flow area is suddenly increased and the pressure in the combustion chamber drops.

The ignition of the gas-generating charge in the combustion chamber is performed with a ready-made igniter. The igniter is activated by a remotely controlled ignition circuit. The power supply is switched to the igniter after a command from the personal computer. After ignition of the gas-generating charge, the combustion products of propellant flow out of the combustion chamber (gas-generating section) into the other sections of the experimental motor and fire the measuring pill. The combustion product gases generated from the propellant sample join the product gases from the gas-generating charge and flow out through the exit and erosive nozzle to the ambient pressure.

Preliminary Results

As mentioned in a previous paper,[17] the index of refraction of the examined propellants at the working microwave frequency is a basic physical quantity that determines the wavelength in propellant, and in this way influences in the first degree the obtained value of burning rate. A special microwave method is developed for the measurement of the index of refraction of all the examined propellants at 35 GHz. The measurement is based on the method of substitution and reflection interferometry. The phase shift introduced by the propellant is counteracted by a calibrated phase shifter to reset destructive interference. Measurements were performed with at least three different thicknesses of propellants. Calculations included multiorder reflections. The indexes of refraction for propellants tested are given in Table 1. The largest standard deviation was obtained for the composite propellant B, and it was 2% from three measurements. The main error in these experiments comes from losses in the propellant and diffraction effects.

Before tests in the real motor were conducted, testing with laboratory equipment had been performed to determine the viability of the whole system. The first tests were performed with the complete transmission microwave installation and the test motor. In these tests, the measuring pill was replaced with a tube, with a conical internal bore. Simulation of propellant regression is obtained as this tube is moved through the covering, at that place where the microwave signal is passing. These tests prove that transmission interferometry and data reduction software can determine the moving rate of a surface, in this case a solid cone.

Burning-Rate Results

Several burning-rate measurements were performed at atmospheric pressure. Tests were performed with three different propellant formulations, with the combustion chamber open to the atmosphere. The conditions for transmission of the microwave signal were the same as in the high-pressure tests. Under these conditions the regression rate is constant because the propellant samples burn at a steady pressure. The results of these experiments for different types of propellants are shown in Fig. 5.

Based on the successful results of all these preliminary experiments, the burning rates of the three different composite propellant formulations at an initial temperature of 293 K were measured using transmission microwave interferometry. The characteristics of propellants that were examined are listed in Table 1. The base burning rates of the propellants are presented in Figs. 6–8. All of the data were correlated with the Saint–Robert's law. The tests were performed with the erosive nozzle closed.

The results of erosive burning are presented in Figs. 9–11, where ε is expressed as a function of G. The erosion ratio is the ratio of measured burning rate during a test with a gas flow over the burning surface and the base burning rate, under the same conditions (combustion pressure and initial propellant temperature). The base burning rates are those of Figs. 6–8. Both nozzles were opened in these tests.

The burning rate vs pressure obtained for the composite propellant A is shown in Fig. 6. Burning rate was measured in a pressure range from 3 to 11 MPa. A total of five tests were performed. Separate tests are represented with different symbols. The gas-generating charges were made from the same propellant as the measuring pill. The measuring pills had stable burning in all conditions. One test has been performed at a constant pressure of 9 MPa, with a special gas-generating charge with neutral burning surface development. This propellant generates high-temperature gas products (over 3000 K), which served to examine the test motor in difficult working conditions.

The composite propellant B was examined in a pressure range from 3 to 12 MPa with six tests. Three tests were performed with gas-generating charges with neutral burning surface development, and they had almost constant burning pressures. The measured burning rate vs pressure is shown in Fig. 7. Separate tests are represented with different symbols. The experiments were done with gas-generating charges made from the same propellant as the measuring pill.

The burning rate of composite propellant C was examined in a pressure range from 4 to 12 MPa. The measured burning rate vs pressure is shown in Fig. 8, where results of separate tests are reported with different symbols. A total of seven experiments were performed. The experiments were performed with gas-generating charges made from the same propellant as the measuring pill.

The erosive burning rate of propellant A is measured in two groups of experiments. Three tests were performed in the first

Table 1 Propellant data

Propellent characteristics	Propellant type		
	A	*B*	*C*
Composition	PVC binder/AP/Al	PVC binder/AP/Al	PVC binder/AP/Al/catalyst
Weight percent	20.25/69.75/10	24.5/75/0.5	21.5/75/0.5/3
Average particle size of filler, μm	73	242	13
Flame temperature of propellant gas, K	3180	2630	2870
Propellant density, kg/m^3	1760	1680	1735
Index of refraction	1.964	1.96	1.968

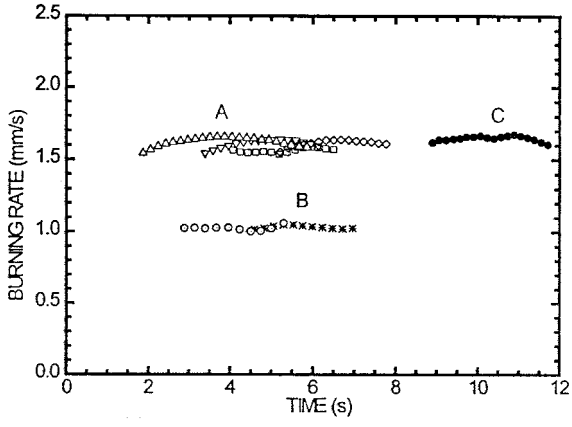

Fig. 5 Burning-rate results at atmospheric pressure.

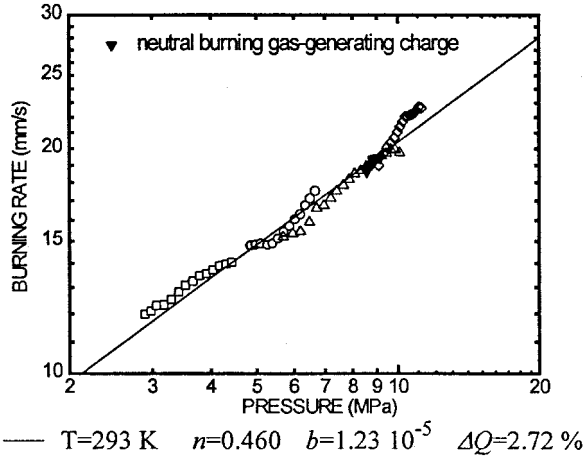

Fig. 6 Burning-rate results of propellant *A*.

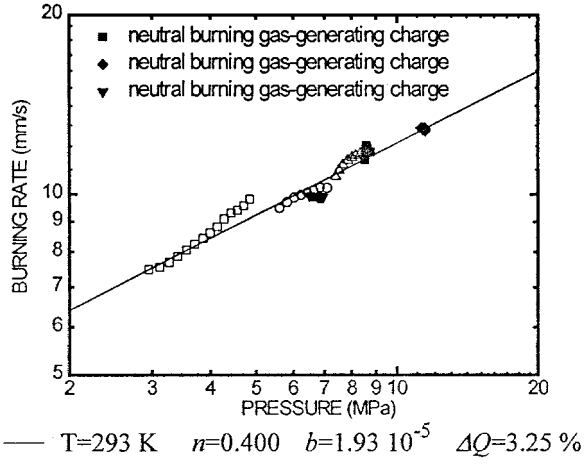

Fig. 7 Burning-rate results of propellant *B*.

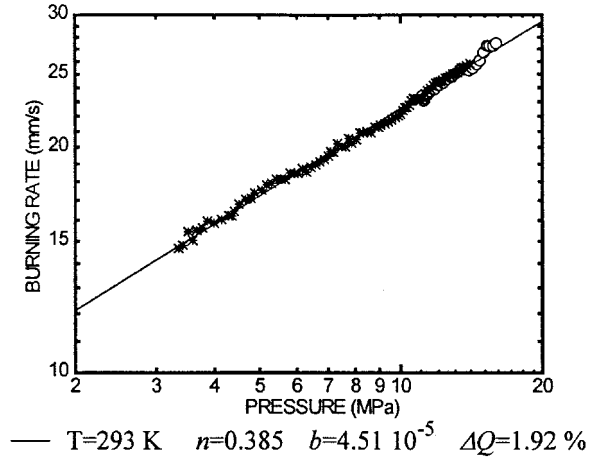

Fig. 8 Burning-rate results of propellant *C*.

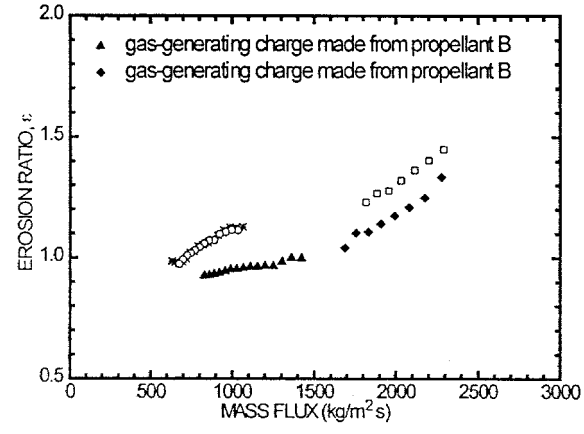

Fig. 9 Erosive burning-rate results of propellant *A*.

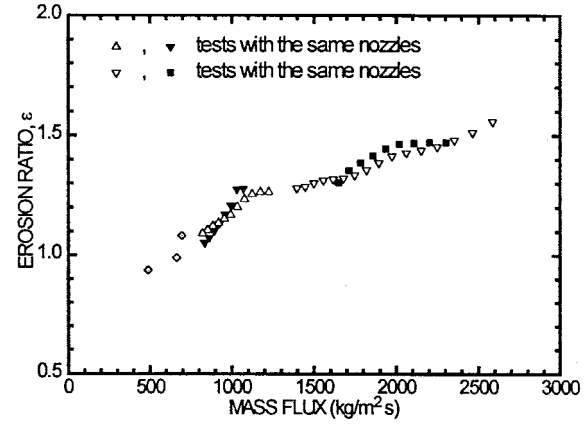

Fig. 10 Erosive burning-rate results of propellant *B*.

group of experiments with the gas-generating charge made from the same propellant formulations used in the measuring pill. Two tests were performed in the second group of experiments. These tests were performed with the gas-generating charge made from composite propellant *B*, which has a much lower flame temperature than the propellant gas. The results are shown in Fig. 9. Results of separate tests are represented with different symbols. The agreement betwen results of two tests under the same conditions and with the same nozzles, done at the first group of experiments, was good. The results from the second group of experiments showed that the erosive burning rate was lower at the same mass flux. The difference is a result of the lower flame temperature of the gas-generating charge.

The results of the erosive burning rate obtained for composite propellant *B* are shown in Fig. 10. Five tests are shown in two pairs done with the same nozzles. The results of these pairs are in good agreement. Results of separate tests are represented with different symbols.

The composite propellant *C*, which contains 3% of catalyst in its formulation (Sicomin-Rot K-3130 S manufactured by BASF), was examined in a mass flux range from 500 to 9000 kg/m^2 s. In total, nine tests were performed with gas-generating charges from the same propellant as the test samples. The results are shown in Fig. 11. Results of separate tests are represented with different symbols. Pairs of tests, done with

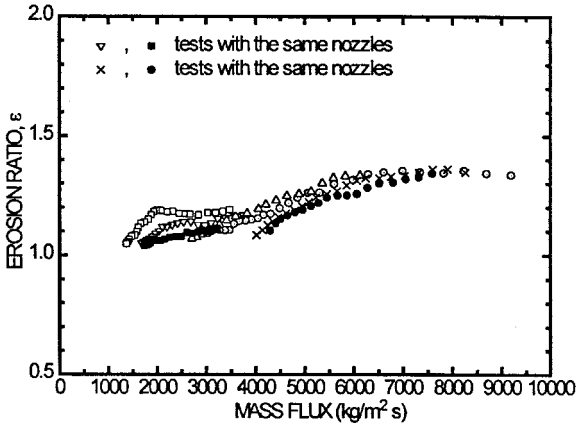

Fig. 11 Erosive burning-rate results of propellant *C*.

the same pairs of nozzles, have shown good agreement between the results.

Conclusions

An experimental apparatus has been designed for measuring the burning rates of solid propellants under wide ranges of pressures and gas flow over the burning surface, in laboratory conditions similar to those in real rocket motors. Numerous tests, which have been performed on composite propellants, have proved that the test motor design and microwave installation are capable of sustaining a large number of tests over a wide range of pressures. The whole microwave installation, except for the horn lens antenna, is removed from the test zone and protected from possible destruction during tests. The base and erosive burning rates of three composite propellant formulations are presented in this paper. This paper shows that transmission microwave interferometry can be successfully used for measuring both the base and erosive burning rate of solid rocket propellants. Conditions in the combustion chamber are closer to those prevailing in a rocket chamber, as the high pressure is generated by hot combustion gases, and the burning rate is measured on a center-perforated cylindrical grain.

References

[1]Kreidler, J. W., "Erosive Burning: New Experimental Techniques and Methods of Analysis," AIAA Paper 64-155, Jan. 1964.

[2]Hsieh, W. H., Char, J. M., Zanotti, C., and Kuo, K. K., "Erosive and Strand Burning of Stick Propellants, Part I: Measurements of Burning Rates and Thermal Wave Structures," *Journal of Propulsion and Power*, Vol. 6, No. 4, 1990, pp. 392–399.

[3]King, M. K., "Erosive Burning of Composite Solid Propellants: Experimental and Modeling Studies," *Journal of Spacecraft and Rockets*, Vol. 16, No. 3, 1979, pp. 154–162.

[4]Razdan, M. K., and Kuo, K. K., "Measurements and Model Validation for Composite Propellants Burning Under Cross Flow of Gasses," *AIAA Journal*, Vol. 18, No. 6, 1980, pp. 669–677.

[5]Razdan, M. K., "Erosive Burning Study of Composite Solid Propellants by the Reacting Turbulent Boundary-Layer Approach," Ph.D. Dissertation, Dept. of Mechanical Engineering, Pennsylvania State Univ., University Park, PA, 1979.

[6]Gordon, J. C., Dutereque, J., and Lengelle G., "Solid-Propellant Erosive Burning," *Journal of Propulsion and Power*, Vol. 8, No. 4, 1992, pp. 741–747.

[7]Green, L., "Erosive Burning of Some Composite Solid Propellants," *Jet Propulsion*, Vol. 24, No. 1, 1954, pp. 9–15.

[8]Dickinson, L. A., Jakson, F., and Odgers, A. L., "Erosive Burning of Polyurethane Propellants in Rocket Engines," *8th Symposium (International) on Combustion*, Williams and Wilkins, Baltimore, MD, 1962, pp. 754–759.

[9]Koch, B., "Reflexion de Micro-Ondes par des Phenomenes de Detonation," *Contes Rendues Academie des Sciences Paris*, Vol. 236, 1953, pp. 661–663.

[10]Johnson, D. L., "Microwave Measurement of the Solid Propellant Burning Rates," Giannini Controls Corp., Duarte, CA, July 1962.

[11]Dean, D. S., and Green, D. T., "The Use of Microwaves for the Detection of Flaws and Measurement of Erosion Rates in Materials," *Journal of Scientific Instruments*, Vol. 44, No. 9, 1967, pp. 699–701.

[12]Wood, H. L., O'Brien, W. F., and Dale, C. B., "Measurement of Solid Propellant Burning Rates Employing Microwave Techniques," Chemical Propulsion Information Agency Publication 383, 1983.

[13]Gittins, J., Gould, R. D., Penny, P. D., and Wellings, P. C., "Solid Propellant Combustion Instability," *Journal of the British Interplanetary Society*, Vol. 25, No. 6, 1972, pp. 597–605.

[14]Alkidas, A., Clary, A., Giles, G., and Shelton, S., "Measurement of Steady State and Transient Solid Propellant Burning Rates with Microwaves," Georgia Inst. of Technology, U.S. Air Force Office of Scientific Research, Final Rept. 70-1934, Atlanta, GA, Dec. 1973.

[15]Strand, L. D., Schultz, A. L., and Reedy, G. K., "Microwave Doppler Shift Technique for Determining Solid Propellant Transient Regression Rates," *Journal of Spacecraft and Rockets*, Vol. 11, No. 2, 1974, pp. 75–83.

[16]Strand, L. D., Magiawaia, K. R., and McNamara, R. P., "Microwave Measurement of the Solid Propellant Pressure-Coupled Response Function," *Journal of Spacecraft and Rockets*, Vol. 17, No. 6, 1980, pp. 483–488.

[17]Bozic, V. S., Blagojevic, D. D., and Anicin, B. A., "Measurement System for Determining Solid Rocket Propellant Burning Rate Using Reflection Microwave Interferometry," *Journal of Propulsion and Power*, Vol. 13, No. 4, 1997, pp. 457–467.

[18]Anicin, B. A., Jojic, B., Blagojevic, D., Adzic, M., and Milosavljevic, V., "Flame Plasma and the Microwave Determination of Solid Propellant Regression Rates," *Combustion and Flame*, Vol. 64, No. 5, 1986, pp. 309–319.

[19]Lashinsky, H., "Plasma Physics Laboratory TM 177," Princeton Univ., Princeton, NJ, 1963.

[20]Savitzky, A., and Golay, J. E. M., "Smoothing and Differentiation of Data by Simplified Least Squares Procedures," *Analytical Chemistry*, Vol. 36, No. 8, 1964, pp. 1627–1639.

[21]Waesche, R. H. W., and O'Brien, W. F., "Evaluation of Techniques for Direct Measurement of Burning Rates in Nozzleless Motors," 24th JANNAF Combustion Meeting, Chemical Propulsion Information Agency, Publication 476, 1987.